Chirukandath Gopinath
Vasanthi Mowat

Atlas of Toxicological Pathology

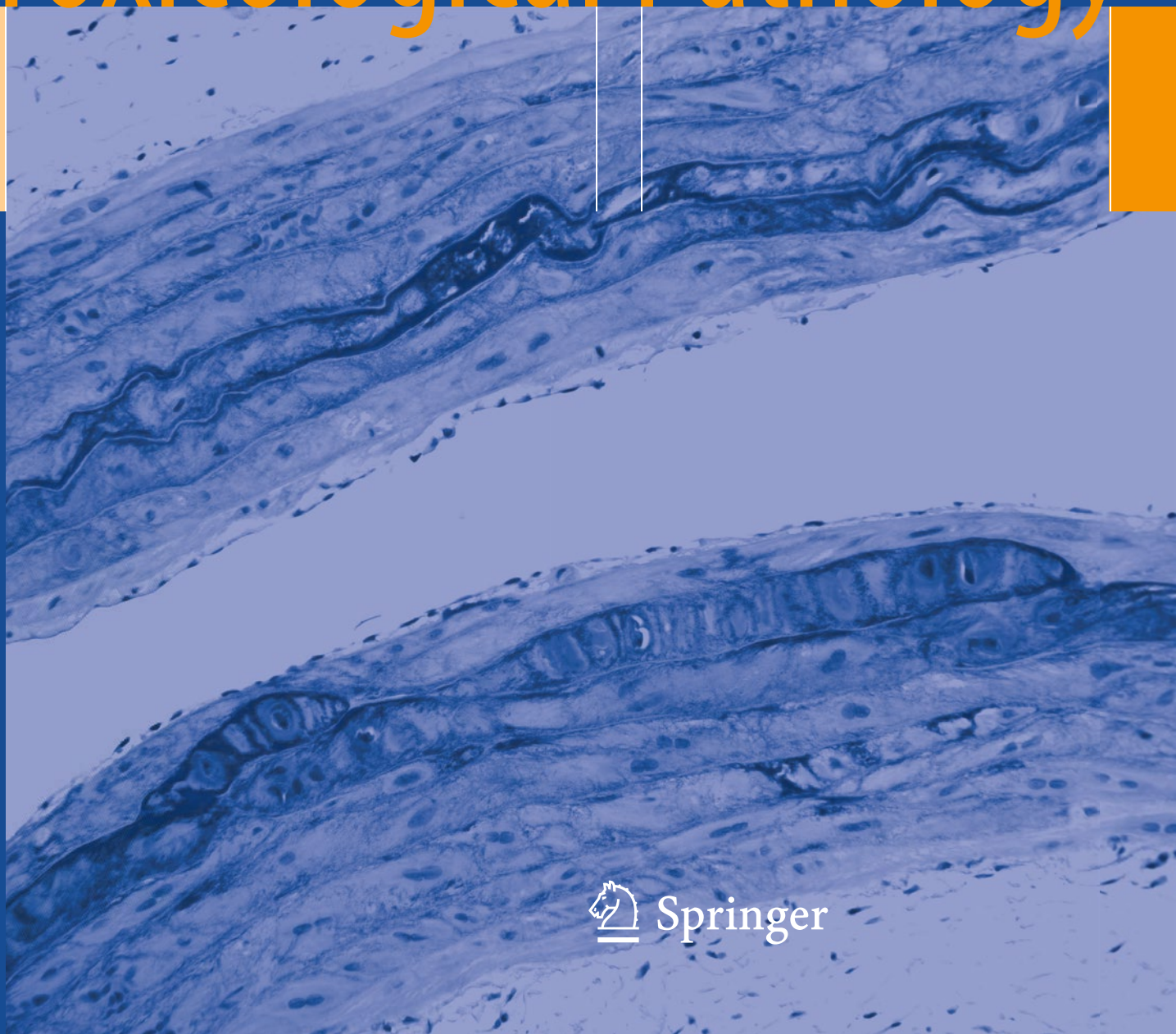

Springer

Atlas of Toxicological Pathology

Chirukandath Gopinath
Vasanthi Mowat

Atlas of Toxicological Pathology

Springer

Chirukandath Gopinath
Consultant in Toxicology and Pathology
Cambridgeshire
UK

Vasanthi Mowat
Huntingdon Life Sciences
Cambridgeshire
UK

ISBN 978-1-62703-997-0 ISBN 978-1-62703-998-7 (eBook)
DOI 10.1007/978-1-62703-998-7
Springer New York Heidelberg Dordrecht London

Library of Congress Control Number: 2014937893

© Springer Science+Business Media New York 2014
This work is subject to copyright. All rights are reserved by the Publisher, whether the whole or part of the material is concerned, specifically the rights of translation, reprinting, reuse of illustrations, recitation, broadcasting, reproduction on microfilms or in any other physical way, and transmission or information storage and retrieval, electronic adaptation, computer software, or by similar or dissimilar methodology now known or hereafter developed. Exempted from this legal reservation are brief excerpts in connection with reviews or scholarly analysis or material supplied specifically for the purpose of being entered and executed on a computer system, for exclusive use by the purchaser of the work. Duplication of this publication or parts thereof is permitted only under the provisions of the Copyright Law of the Publisher's location, in its current version, and permission for use must always be obtained from Springer. Permissions for use may be obtained through RightsLink at the Copyright Clearance Center. Violations are liable to prosecution under the respective Copyright Law.
The use of general descriptive names, registered names, trademarks, service marks, etc. in this publication does not imply, even in the absence of a specific statement, that such names are exempt from the relevant protective laws and regulations and therefore free for general use.
While the advice and information in this book are believed to be true and accurate at the date of publication, neither the authors nor the editors nor the publisher can accept any legal responsibility for any errors or omissions that may be made. The publisher makes no warranty, express or implied, with respect to the material contained herein.

Printed on acid-free paper

Humana Press is a brand of Springer
Springer is part of Springer Science+Business Media (www.springer.com)

Preface

This colour atlas follows in the footsteps of the *Atlas of Experimental Toxicological Pathology*, edited and authored by Gopinath, Prentice, and Lewis and published by MTP Press Ltd, Lancaster, UK, in 1987. This atlas is still widely used and is recognised as one of the standard reference texts in this field. This latest version is an update with numerous new illustrations that the authors have collected over the years, and with references and information pertaining to recently developed drug classes, including biologics.

The field of toxicological pathology has expanded vastly, and although several excellent textbooks on toxicological pathology have been published over the past two decades, the authors still feel that this atlas has a significant role to play and will be useful for practising toxicological pathologists of all levels of experience.

Toxicological pathology is a subspeciality of pathology and is a comparatively young profession, dealing mainly with the pathology of laboratory animals used in toxicity studies. As such, it includes a variety of animal species that are used in this field. Different strains of rats, mice, beagle dogs and nonhuman primates form the bulk of animals used in safety assessment studies. Rabbits, hamsters, mini-pigs, guinea pigs, and chickens form a smaller proportion of these studies. Less commonly, domestic animals including goats, sheep, and cattle are also used in these studies. This makes veterinarians, by virtue of their training, ideally suited as candidates for toxicological pathologists.

Toxicity studies are generally driven by protocols designed by various governmental regulatory bodies, mainly from Europe, the USA and Japan. These studies are carried out to assess potential toxicity of the test substances. The test articles may be novel pharmaceuticals, agrochemicals or chemical entities, and include biologics such as vaccines and antibodies.

Toxicity studies are designed with one or more control groups and a few incremental dose levels of the test substance that are selected to represent multiples of the potential exposure levels in humans. The high doses are chosen to induce toxicity in target organs, and lower doses are used to determine no effect levels and no adverse effect levels where possible. With pharmaceuticals, these studies provide information on potential risk during human use and also on side effects during therapy. With chemicals and agrochemicals, these provide data on potential human hazard due to either industrial or environmental exposure. Exposure through either the food chain or the water supply, due to contamination of the environment by use on crops or soil, are also causes for concern.

Toxicity studies are carried out by different routes of administration that mimic expected routes of human exposure. These include dietary, oral, inhalation and parenteral administration. Parenteral routes include subcutaneous, dermal, intradermal or intravenous (bolus or continuous infusion) administration. The duration of the studies varies according to the intended use of the test substance and may vary from a single dose to a few days to lifelong exposure. The aim of all toxicity studies is to assess the potential risk of the test substance to man when in use.

Pathology is an integral part of these studies at termination, as all animals are subject to autopsies and tissue preservation followed by histopathological evaluation and reporting. A full list of organs/tissues is routinely processed from control animals and some or all treated groups, according to the study protocol and using standard operating procedures. By

comparing the results between treated and control groups, the pathologist identifies treatment-related changes and target organs. A sound knowledge of the background pathology of the strain/species of the animals used and of the induced lesions associated with different compound classes is essential for accurate evaluation and interpretation of these studies. This atlas includes a few common spontaneous lesions, but the illustrations are primarily of induced lesions, mostly of a nonneoplastic nature. A few examples of induced rodent tumours from carcinogenicity studies are included. The atlas is organised into different chapters based on systemic pathology. Each chapter has illustrations with legends that briefly identify the changes and a text that explains the changes with references wherever possible. Most of the illustrations are recently sourced from the authors' own collections. A small number that have been used from the previous atlas are acknowledged. The atlas includes some rare examples of unique lesions found during toxicity studies over many years.

It is hoped that the atlas will be useful as a bench reference for practising pathologists and will also be used as a reference text by other experts from related fields.

Cambridgeshire, UK Chirukandath Gopinath
Cambridgeshire, UK Vasanthi Mowat

Acknowledgement

We are very grateful to Huntingdon Life Sciences for the wealth of experience we have gained here and for the opportunity to publish this atlas.

We have followed the general pattern/theme of a previous atlas on a similar topic, and we are thankful to D.E. Prentice and D.J. Lewis (editors/authors of *Atlas of Experimental Toxicological Pathology*) for their general approval and encouragement for the present book and their permission to reuse some of the photographs.

We are indebted to many people who have helped us in the preparation of this atlas, especially the pathology group at HLS. In particular, we would like to acknowledge David Bell, Dianne Creasy, James Cartwright, and Andrew Pilling for variously helping with photography, providing photographs, and reviewing sections of the manuscript.

Lastly, we thank our partners and children for their unfailing understanding and patience during the preparation of this atlas. Without their support, this project would not have been possible.

Contents

1 The Cardiovascular System

Induced myocardial lesions such as myocardial degeneration/necrosis, haemorrhage, and fibrosis are described with illustrations. The mechanisms underlying myocardial injuries are discussed. Changes occurring as a result of exaggerated pharmacological actions and those occurring because of direct toxicity are included. Other changes discussed include myocardial hypertrophy, coronary and myocardial vascular lesions, and changes to the valves and pericardium. Lesions affecting peripheral vessels are also described. Drug-induced vascular injury, inflammatory and degenerative changes affecting vessel walls, thrombosis, mineralisation, and atherosclerosis are illustrated.

1.1 Heart

1.1.1 Introduction

Spontaneous cardiovascular injury is somewhat rare in routine toxicity studies. However, cardioactive drugs target the heart quite regularly in toxicity studies. Several good reviews of drug-induced cardiac lesions exist [1–4]. Many cardioactive drugs and some chemicals and metals are known to produce myocardial injuries. Myocardial toxicity induced by cytotoxic agents usually produces widespread and multifocal lesions, and pharmacologically mediated changes are mostly focal with specific anatomical locations, leaving large areas of the myocardium unaffected [1, 5]. Routine screening can sometimes miss lesions in the myocardium owing to restricted sampling. Accurate detailed dissection techniques and sampling are essential to avoid missing vital information/lesions [6]. The myocardium on rare occasions reveals lesions that are secondary to renal failure, stress, or certain central nervous system lesions. Functional tests employed do not always correlate with pathologic changes in the myocardium in toxicity studies. The use of biomarkers, notably troponins, is valuable in monitoring myocardial lesions [7, 8]. An integrated approach evaluating a number of cardiovascular parameters allows detection of minimal early changes and thorough characterisation of any lesions [9].

Induced myocardial lesions are summarised as:

- Myocardial degeneration/necrosis
- Myocardial vacuolation
- Myocardial haemorrhage
- Myocardial pigmentation
- Myocardial calcification
- Myocardial hypertrophy
- Valvular changes
- Myocardial vascular changes
- Pericarditis

Catecholamines and a few other cardioactive agents produce myocardial injuries through exaggerated pharmacological responses. Myocardial fibres are excessively

C. Gopinath, V. Mowat, *Atlas of Toxicological Pathology*,
DOI 10.1007/978-1-62703-998-7_1, © Springer Science+Business Media New York 2014

stimulated, resulting in increased energy and oxygen demand. Functional stimulation causes transmembrane calcium influx, which enhances muscle activity. Vasodilation results in a localised drop in coronary blood pressure, reduced perfusion time, perturbation of transmural blood flow, and development of subendothelial steal phenomenon and set up reflex tachycardia. All these in turn contribute to local ischaemia leading to myocardial degeneration and necrosis in the most vulnerable sites, such as subendocardial foci in papillary muscles and left ventricles. It is interesting to note that cardiostimulants (resulting in tachycardia) and cardioinhibitors (causing extreme bradycardia) can both induce similar myocardial lesions owing to local ischaemia at very high doses (personal observation). Dogs appear to be more susceptible than rodents to cardiotoxicity.

Histologically, small foci or groups of myocardial fibres show swelling, increased eosinophilia of the sarcoplasm, and loss of striation (Figs. 1.1 and 1.2). Frequently this is accompanied by increased granularity, fragmentation, and development of contraction bands. Affected fibres reveal transverse bands that are condensed contractile materials (Fig. 1.3). Preparation artefacts can also reveal focal myocardial fibres with increased eosinophilia (Fig. 1.4). The degenerating fibres occasionally show intracytoplasmic

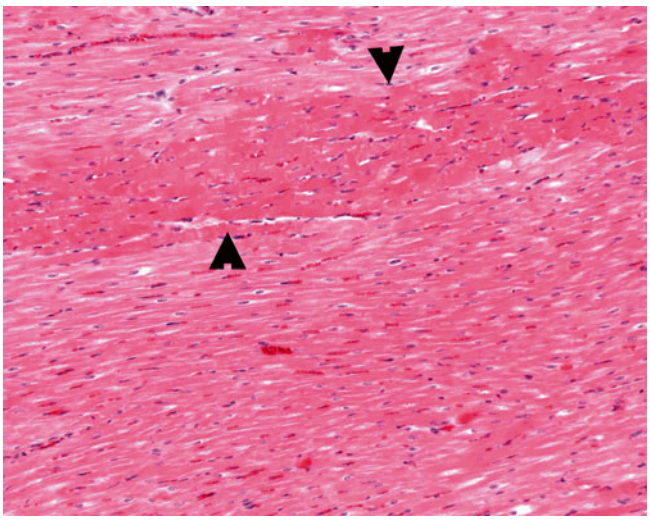

Figure 1-1. Myocardial degeneration, left ventricle, in a dog treated with a cardioactive agent. Affected fibres (*arrowheads*) appear more eosinophilic with loss of striations. Haematoxylin and eosin (H&E).

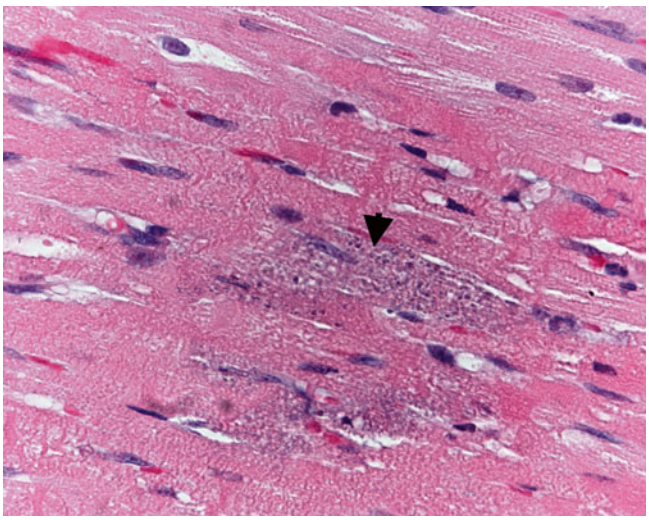

Figure 1-2. Myocardial degeneration and calcification, left ventricle, in a dog treated with a cardioactive agent. Affected fibres reveal increased eosinophilia and contraction bands. A few fibres reveal basophilic granular intracytoplasmic deposits (*arrowhead*) representing calcium. H&E.

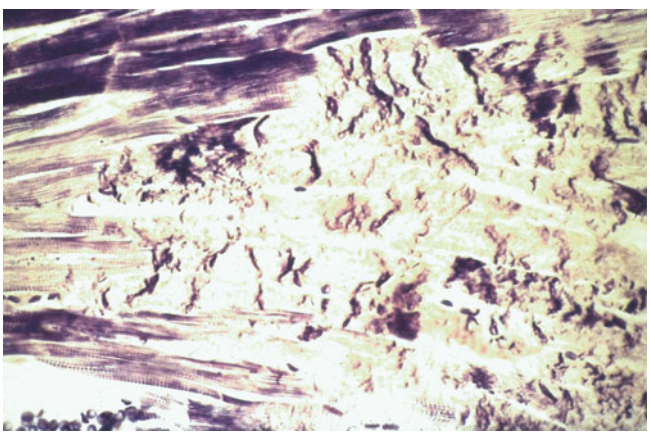

Figure 1-3. Myocardial necrosis, left ventricle, in a dog treated with isoprenaline. Affected fibres show loss of staining (striations), but show several contraction bands. Phosphotungstic acid haematoxylin (PTAH).

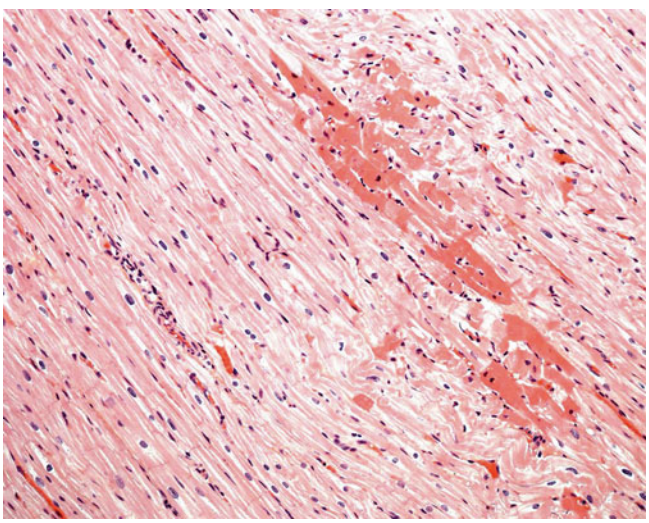

Figure 1-4. Eosinophilic shrunken myocardial fibres, untreated dog heart, represent a preparation artefact. H&E.

granular basophilic calcium deposits (Figs. 1.5 and 1.6). The fibres undergo vacuolation, lysis, and nuclear changes including loss of fibres (Fig. 1.7). Initially a minimal inflammatory response (with notable absence of neutrophil infiltration) is followed by a more marked histiocytic infiltration and, later still, a fibroblastic response (Figs. 1.8 and 1.9). Phosphotungstic acid haematoxylin (PTAH) staining is useful in demarcating degenerative/necrotic lesions in the myocardium (Fig. 1.10). In the early stages (acute), heart-specific enzymes like transaminases, lactate dehydrogenases, creatine phosphokinase, and other cardiac biomarkers such as troponins show elevations in serum, along with changes in the electrocardiogram (ECG) during

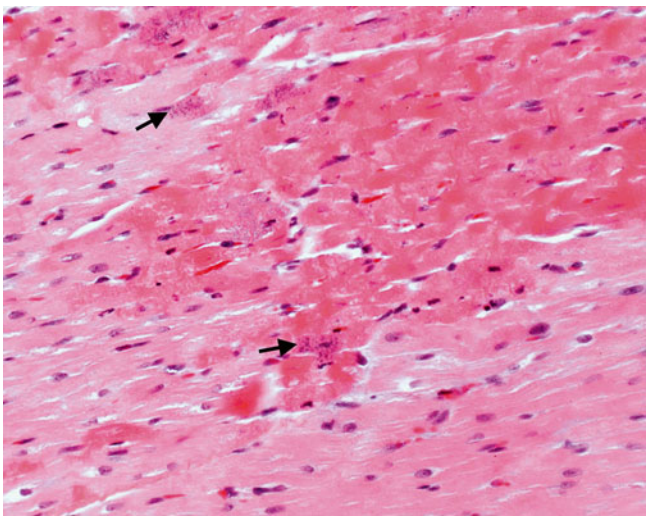

Figure 1-5. Myocardial calcification, left ventricle, in a dog treated with a cardioactive agent. Basophilic intracytoplasmic deposits (*arrows*) represent calcium within degenerating (eosinophilic) fibres. H&E.

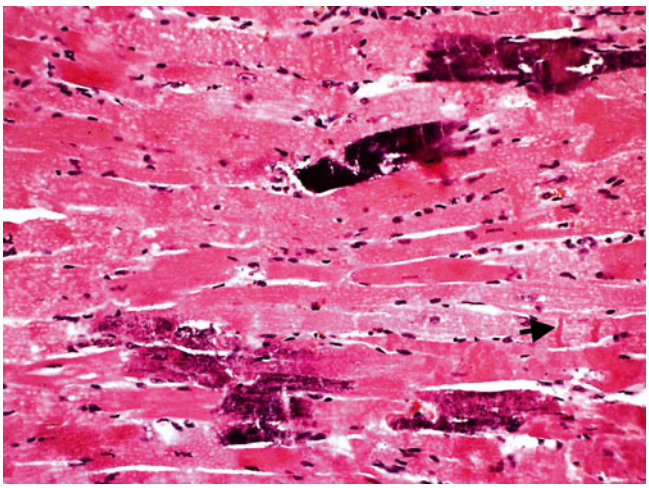

Figure 1-6. Myocardial degeneration and calcification, left ventricle, in a dog treated with a cardioactive agent. Dark basophilic deposits of calcium in the degenerating fibres also show occasional contraction bands (*arrow*). H&E.

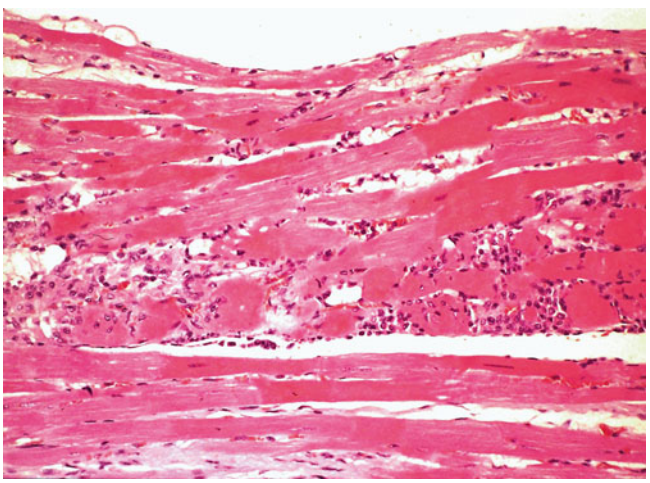

Figure 1-7. Subendocardial myocardial necrosis and vacuolation, left ventricle, in a dog treated with a cardioactive agent reveal vacuolation, minimal inflammatory response, and loss of fibres. H&E.

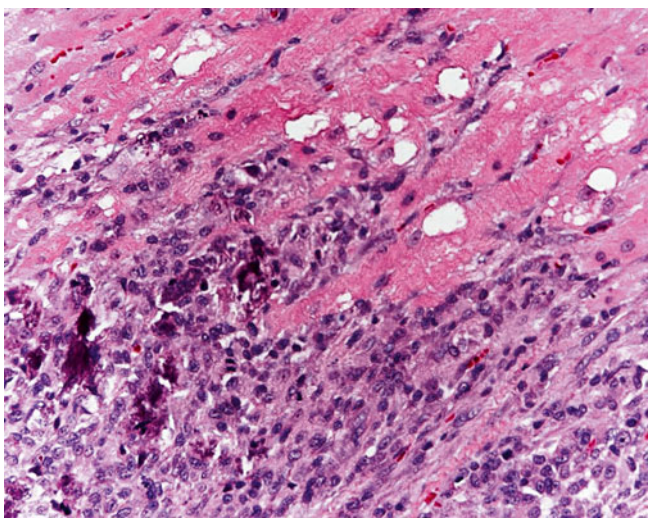

Figure 1-8. Myocardial necrosis, left ventricle, in a dog treated with a cardioactive agent. Extensive fibrohistiocytic response is present. Adjacent fibres show vacuolation and focal calcification. H&E.

the ischaemic stages. In the later stages these are not very helpful in animal studies because levels decline to baseline soon after acute injury [10, 11]. In addition to myocardial necrosis, a number of β-adrenergic stimulants and antihypertensive vasodilators produce subendocardial and intramyocardial haemorrhage (Figs. 1.11 and 1.12). The areas of haemorrhage are frequently accompanied by pigmented macrophages, inflammation, and fibrosis (Fig. 1.13). Areas of fibrosis are a common sequel to myocardial necrosis (Fig. 1.14). Cardioactive drugs in dogs can result in endocardial haemorrhage, inflammation, and fibroblastic proliferation (Figs. 1.15 and 1.16). Haemorrhagic cardiomyopathy in male mice has been induced by a reverse transcriptase inhibitor and was found to be secondary to an induced vitamin K deficiency [12].

Digitoxin and theobromine and antihypertensive agents like minoxidil all can produce vascular lesions, haemorrhage, and myocardial necrosis (Fig. 1.17). These agents induce changes in the right ventricle and

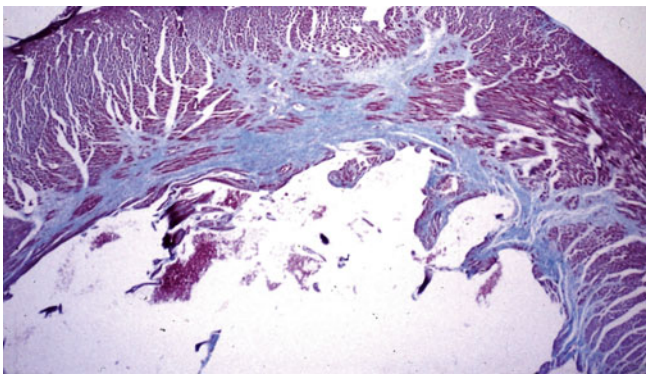

Figure 1-9. Myocardial fibrosis, left ventricle, in a dog treated with a cardioactive agent. Fibroblast proliferation replaces injured myocardial fibres. Trichrome.

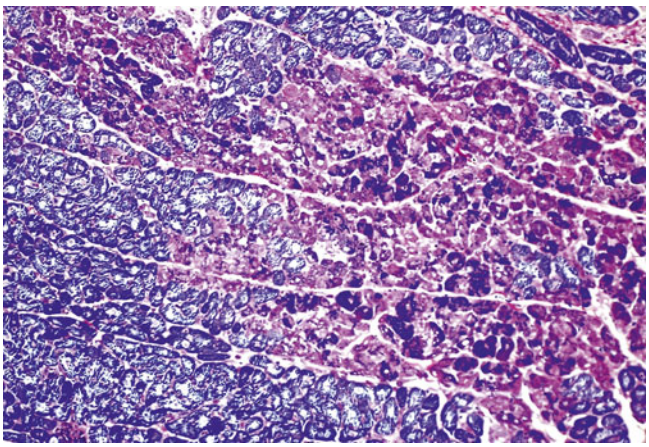

Figure 1-10. Early myocardial degeneration/necrosis, left ventricle, in a dog treated with isoprenaline. Loss of cytoplasmic staining clearly demarcates the lesion. PTAH.

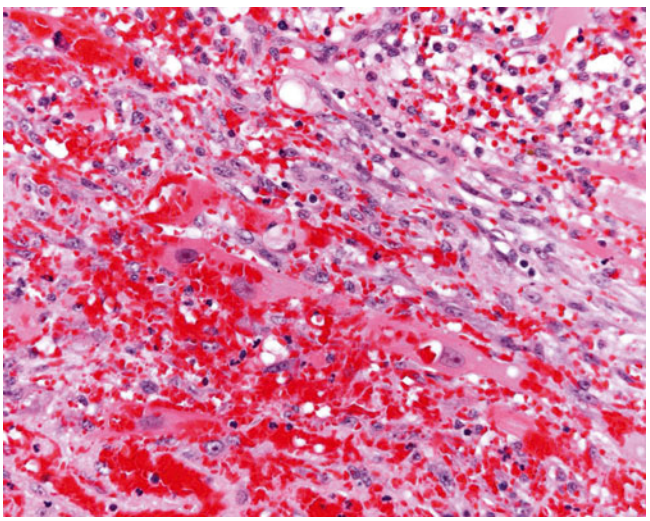

Figure 1-11. Myocardial necrosis and haemorrhage, interventricular septum in a monkey treated with a cardioactive agent. Myocardial necrosis, interstitial haemorrhage, fibroblasts, and inflammation are present. H&E.

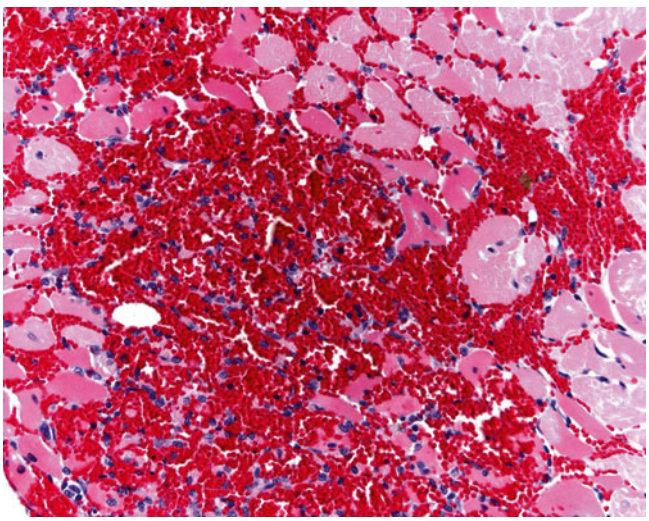

Figure 1-12. Myocardial haemorrhage, left ventricle, in a monkey treated with an antithrombotic agent. Extensive haemorrhage and adjacent fibres are necrotic. H&E.

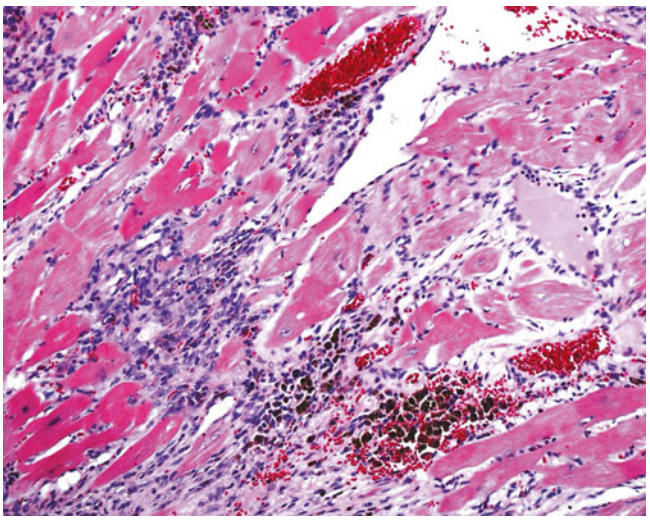

Figure 1-13. Myocardial fibrosis and pigmentation, interventricular septum, in a monkey treated with an antithrombotic agent, reveal areas of fibrosis, haemorrhage, and dark brown pigment. H&E.

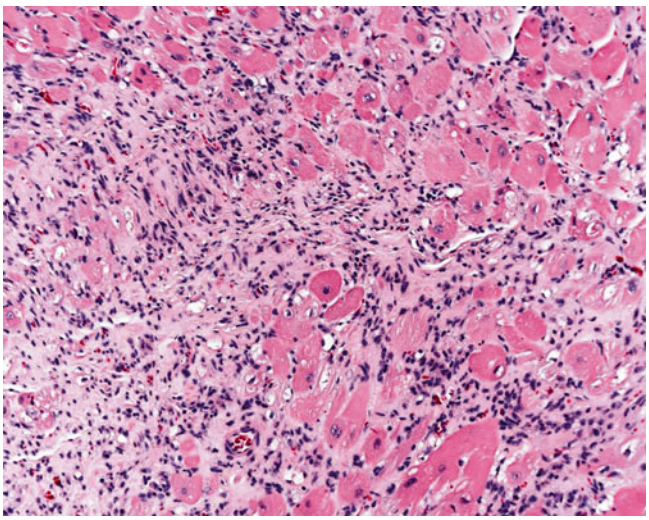

Figure 1-14. Myocardial fibrosis, left ventricle, in a rat treated with a cardioactive agent. Areas of myocardium are replaced by fibrosis. H&E.

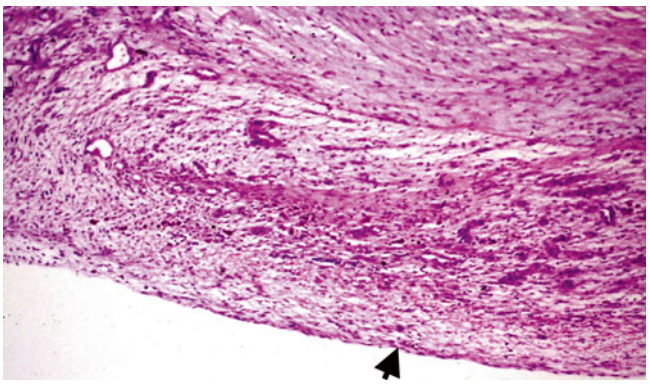

Figure 1-15. Endocardial inflammation, left ventricle, in a dog treated with a cardioactive agent. Endocardium is thickened (*arrow*) and reveals inflammation and early fibroblastic proliferation. H&E.

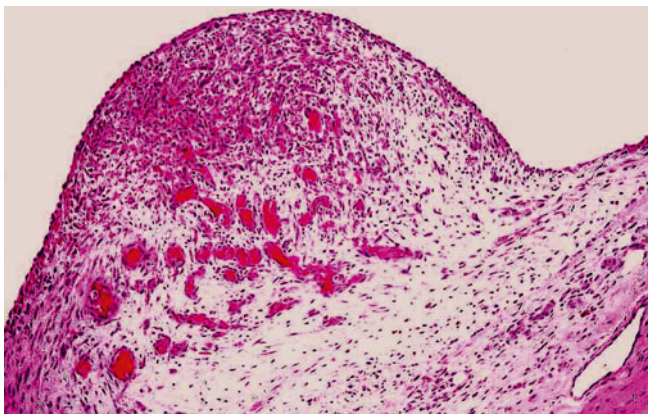

Figure 1-16. Endocardial inflammation, left ventricle, in a dog treated with a cardioactive agent reveals inflammation, neovascularisation, and fibroblastic proliferation. H&E.

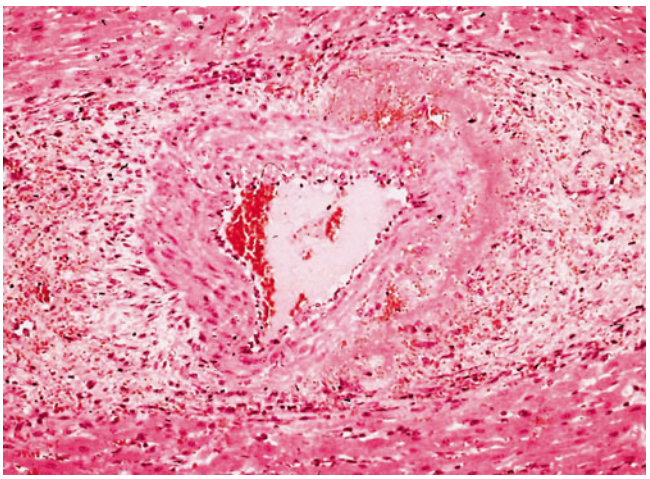

Figure 1-17. Vascular injury, intramyocardial artery, left ventricle, in a dog treated with a vasoactive agent. The artery shows intramural necrosis and haemorrhage and perivascular inflammation, haemorrhage, and fibrosis. H&E.

left ventricles associated with arteritis of the intramural arteries [13]. The affected arteries show medial haemorrhage, fibrinoid necrosis, and inflammation of the media and adventitia [14]. This may progress to thickening of the tunica media and fibrosis and inflammation of the tunica adventitia (Figs. 1.18 and 1.19). Tyrosine kinase receptor inhibitors are associated with myocardial degeneration in the ventricular walls, apex, and interventricular septum when administered to rats (Figs. 1.20 and 1.21) [15]. With the tyrosine kinase inhibitor imatinib, severity of cardiotoxic changes is influenced by arterial blood pressure [16]. Chronic inflammation of the heart base, major blood vessels, and valves has been induced in mice by a phosphodiesterase-4 (PDE-4) inhibitor [17].

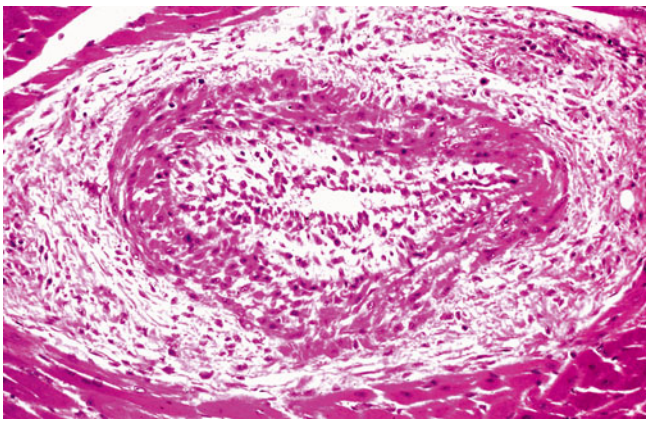

Figure 1-18. Arterial hypertrophy, intramyocardial artery, left ventricle, in a dog treated with a cardioactive agent. Thickening of tunica media, inflammation, and periarteritis are present. H&E (With kind permission from Springer Science + Business Media B.V [1]).

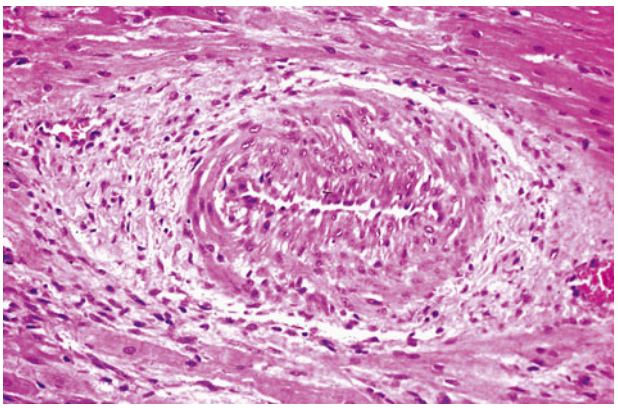

Figure 1-19. Arterial hypertrophy, intramyocardial artery, left ventricle, in a dog treated with a cardioactive agent. Smooth muscle hyperplasia of tunica media and periarterial fibrosis are present. H&E (With kind permission from Springer Science+Business Media B.V [1]).

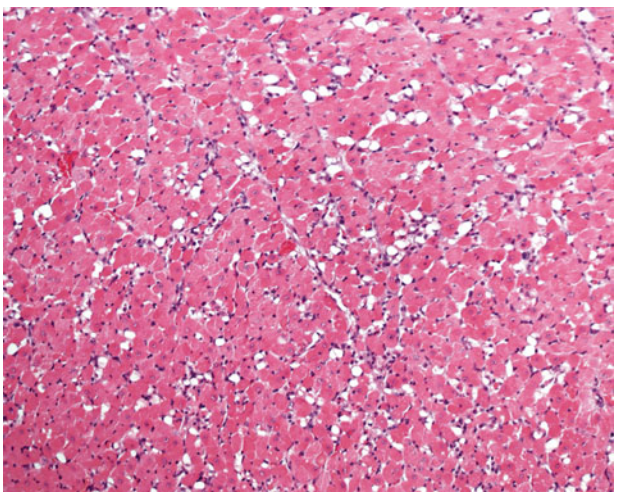

Figure 1-20. Myocardial degeneration, multifocal, interventricular septum, in a rat, shows widespread involvement. H&E.

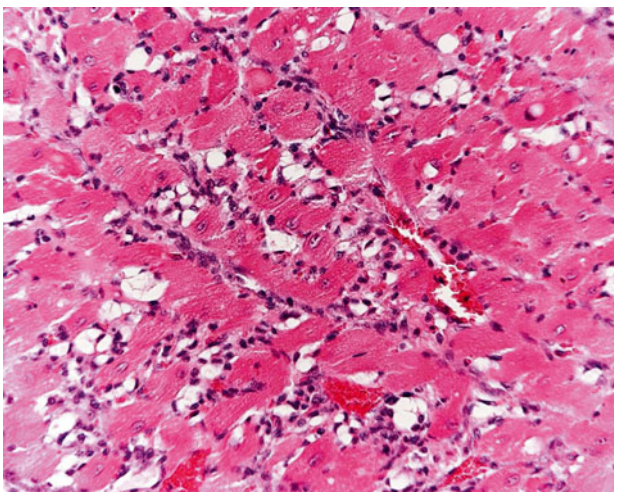

Figure 1-21. Myocardial degeneration, widespread involvement, affecting different areas of myocardium suggests cardiotoxicity. H&E.

Prolonged administration of β-stimulants and other cardioactive agents to rats results in an increase in incidence and severity of spontaneous chronic cardiomyopathy in older rodents, mainly affecting the left ventricle (Figs. 1.22 and 1.23). Therefore, it is important to record severity grades in such studies. In advanced cases marked fibrosis and cardiac dilation occur. Sometimes cartilaginous metaplasia of chordae tendineae and valves develops (Figs. 1.24 and 1.25).

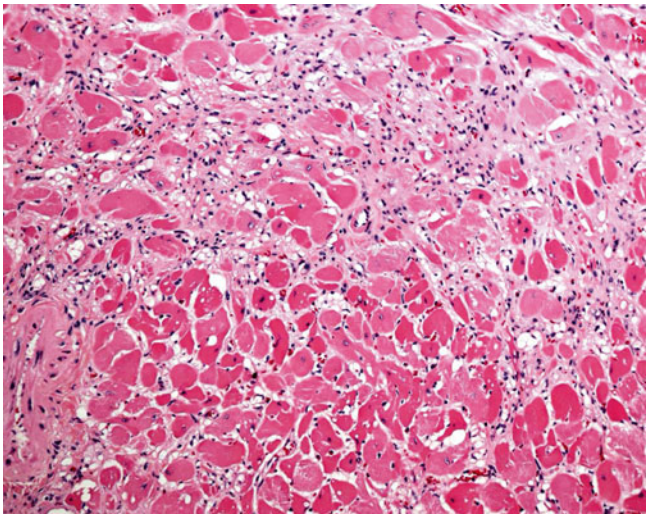

Figure 1-22. Cardiomyopathy, left ventricle, in a rat from a chronic toxicity study with a cardioactive agent. Myocardial degeneration, fibre loss, and fibrosis are present. H&E.

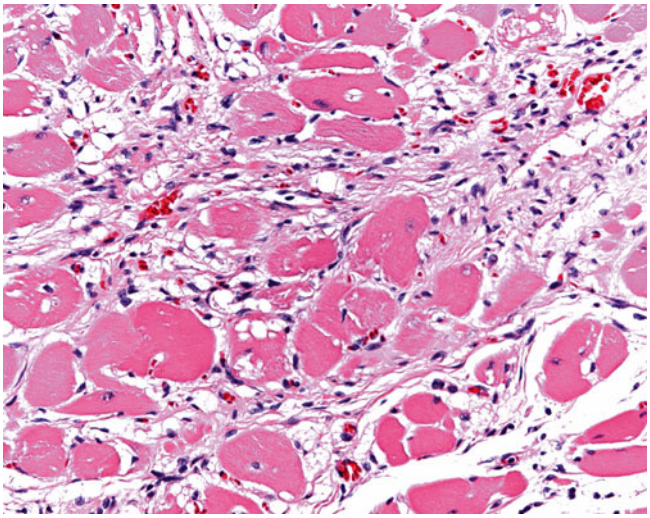

Figure 1-23. Cardiomyopathy, left ventricle, in a rat. Note concurrent appearance of active degeneration/necrosis and fibrous replacement. H&E.

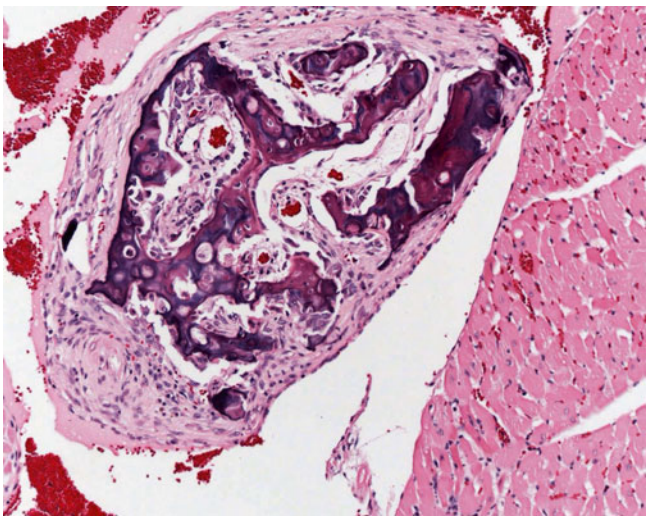

Figure 1-24. Extensive cartilaginous metaplasia, papillary muscle, left ventricle, in a rat from a chronic study with a cardioactive agent. H&E.

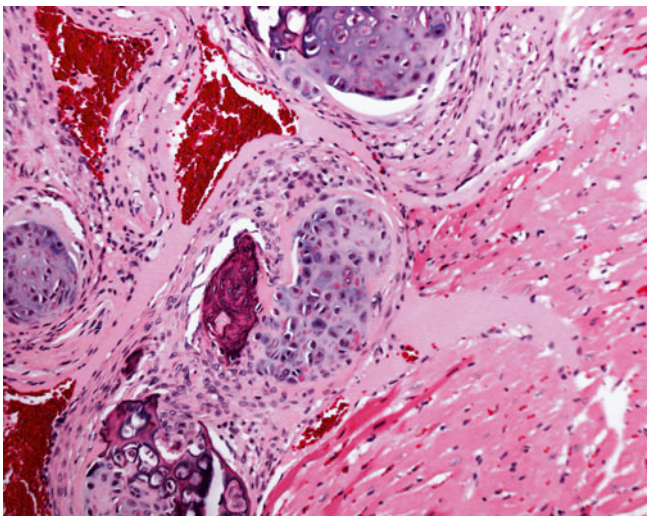

Figure 1-25. Myocardial fibrosis and cartilaginous metaplasia, left ventricle, in a rat with advanced cardiomyopathy. H&E.

Histamine induces multifocal myocardial necrosis of the right ventricle in rabbits. Cobalt salts induce myocardial necrosis and calcification in piglets, affecting mainly the atria. Protein deficiency exaggerates myocardial injury by cobalt; the affected myocardium shows macrophage infiltration, fibrosis, and oedema. Gossypol produces multifocal myocardial vacuolation and necrosis in experimental animals including monkeys (Figs. 1.26 and 1.27) [1, 18]. In pigs gossypol produces ventricular dilation and congestive heart failure. Cyclophosphamide induces haemorrhagic myocardial necrosis in monkeys and dogs. Ionophores like monensin are associated with myocardial vacuolation and necrosis in experimental animals (Figs. 1.28 and 1.29). Rodenticides, fluoroacetates, and 5-fluorouracil are capable of producing multifocal myocardial necrosis [19].

Anthracycline antibiotics like Adriamycin, daunomycin, and doxorubicin induce multifocal myocardial vacuolation, hyalinisation, and loss of fibres [19, 20]. The vacuolation is due to distension of endoplasmic reticulum and t-tubules. Lesions can be associated with fibrosis, oedema, and often cardiac dilation. Adriamycin is cardiotoxic to several species of experimental animals and humans [21]. Rodents are slow to develop Adriamycin-induced toxicity.

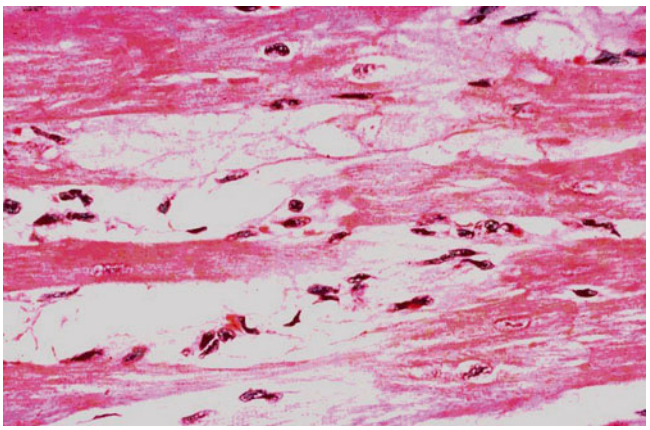

Figure 1-26. Myocardial vacuolation, interventricular septum, in a dog treated with an anticancer agent. Swelling, vacuolation of myocardial fibres, and minimal inflammatory cell infiltration are noted. H&E.

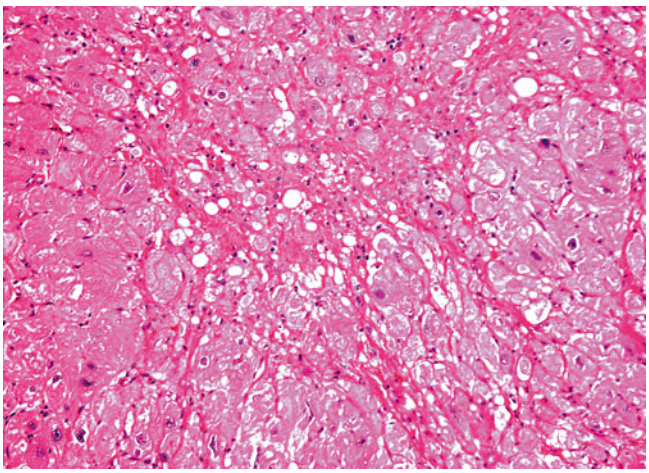

Figure 1-27. Myocardial vacuolation and fibrosis, interventricular septum, in a cynomolgus monkey. Similar lesions at low incidences have been noted in untreated monkeys. H&E.

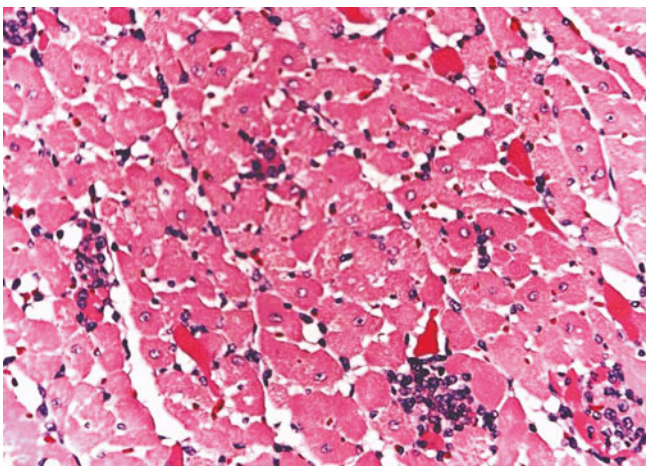

Figure 1-28. Myocardial necrosis, multifocal, right ventricle, in a rat treated with an industrial chemical. Necrotic fibres associated with inflammation are present. H&E.

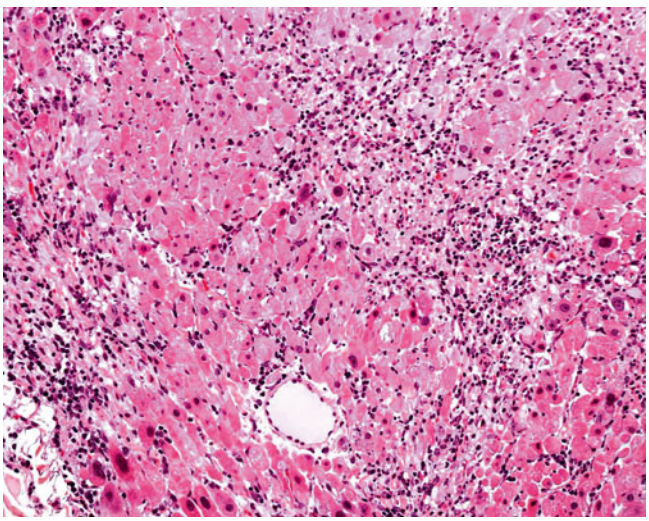

Figure 1-29. Myocardial necrosis, multifocal, interventricular septum, in a monkey treated with a novel pharmaceutical. Areas of necrosis and inflammation are noted. H&E.

Fatty degeneration and myocytolysis are induced in rats given high doses of brominated vegetable oils [1]. Glucocorticoids when given to rats result in lipid accumulation and myocardial degeneration. Cardiac muscles can develop phospholipidosis, manifesting as vacuolation (confirmed as phospholipidosis by electron microscopy), when exposed to agents like chloroquine. Administration of a food pigment, Brown FK, to rats results in lipofuscin-like pigment deposition along with focal necrosis. Hypervitaminosis D causes metastatic calcification of the myocardium and myocardial arteries and aorta (Figs. 1.30 and 1.31). Hypothyroidism and diabetes mellitus can cause fat accumulation in the myocardium. Allylamine also causes fatty degeneration and myocardial necrosis [22].

Right atrial damage including fibrosis, haemorrhage, and inflammation occurs in treatment with minoxidil and hydralazine [1, 19]. Digitoxin also causes haemorrhagic lesions in the right atrium (Fig. 1.32). Subendocardial haemorrhage is seen in dogs with renal failure and uraemia.

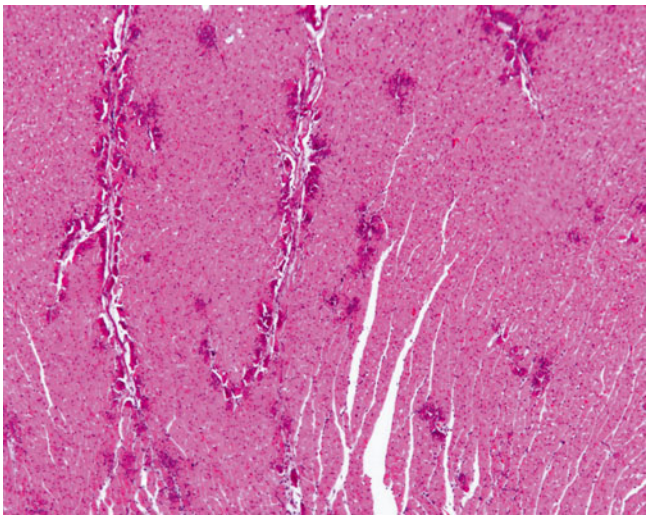

Figure 1-30. Myocardial calcification, multifocal, right ventricle, in a rat treated with a vitamin D analogue. Multifocal deposits of calcium, mostly adjacent to vessels, are present. H&E.

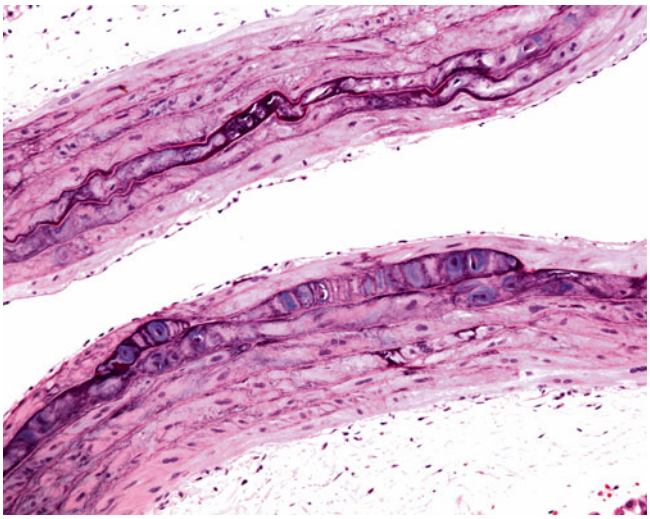

Figure 1-31. Calcification and cartilaginous metaplasia, aorta, in a rat from a chronic toxicity study with a vitamin D analogue. Elastic fibres in aortic wall reveal mineralisation along with cartilaginous metaplasia. H&E.

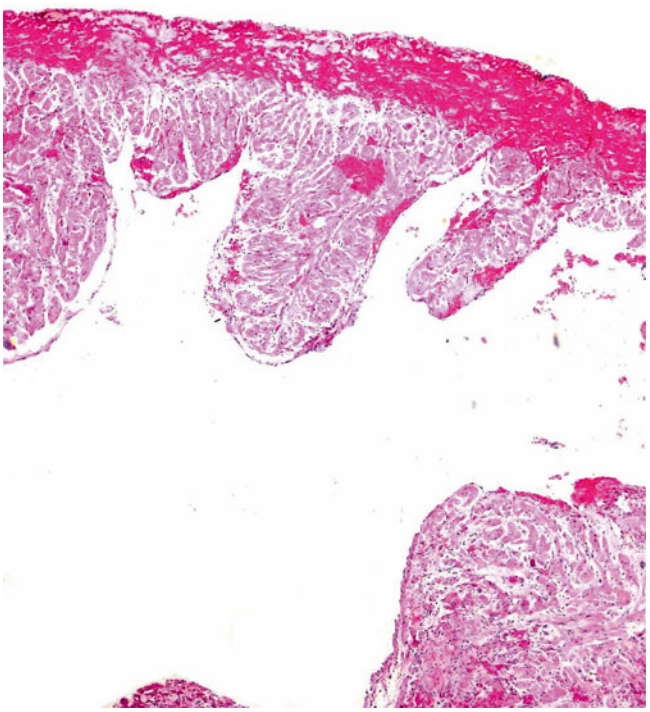

Figure 1-32. Myocardial haemorrhage, right atrium, in a monkey treated with a novel pharmaceutical. H&E.

Myocardial hypertrophy can be induced in response to mechanical, haemodynamic, hormonal, and physiological stimulation. Systemic hypertension produces left ventricular hypertrophy. Hypertrophy can also be physiological, as seen in athletes and racehorses, owing to increased exercise and in females during pregnancy. Chronic exposure to catecholamines and administration of thyroxine, growth hormone, testosterone, and anabolic steroids cause myocardial hypertrophy. Oxfenicine produces an increase in heart weight in dogs and rats [23]. Troglitazone causes myocardial hypertrophy in rodents but not in monkeys [24]. Some other related antidiabetic agents are known to result in myocardial hypertrophy in monkeys. Myocardial hypertrophy can be localised, affecting only a few fibres as seen in areas adjacent to chronic myocardial lesions, or it can affect the entire chamber(s). Certain calcium channel blockers given to dogs cause myocardial hypertrophy. The affected fibres appear larger and broader with large vesicular nuclei (Fig. 1.33). A growth hormone analogue resulted in visible enlargement of the heart in rats (hypertrophy) without producing any frank microscopic changes in the myocardium (Fig. 1.34). Arsenic, when given to mice in the drinking water, produces hypertension and left ventricular concentric hypertrophy [25].

Endothelin antagonists can induce arteritis of coronary arteries with thrombosis. Pericarditis, vasculitis, and myocarditis have been induced in dogs by an immunomodulator. Muramyl peptide given to dogs induces pericarditis and myocarditis (Fig. 1.35). Epicarditis has been induced by a sweetener in dogs. Treatment of dogs with certain immunostimulants has produced vasculitis, with endothelial proliferation and thrombosis with associated myocardial necrosis (Fig. 1.36). In later stages the thrombi cause occlusion and undergo recanalisation (Figs. 1.37–1.39) [1].

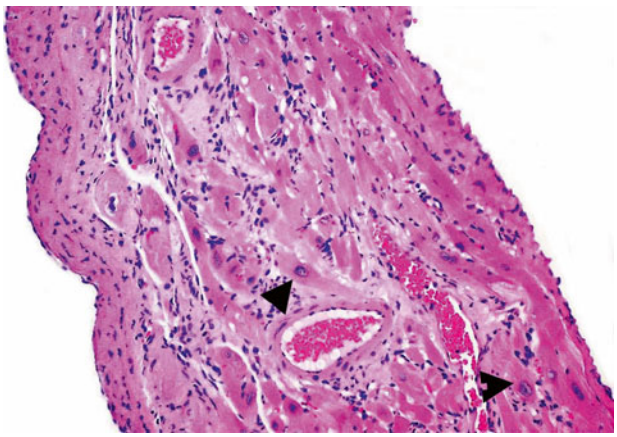

Figure 1-33. Myocardial hypertrophy, focal, right ventricle, in a monkey. Affected fibres (*arrowheads*) are larger with large open nuclei. There is some interstitial fibrosis. H&E.

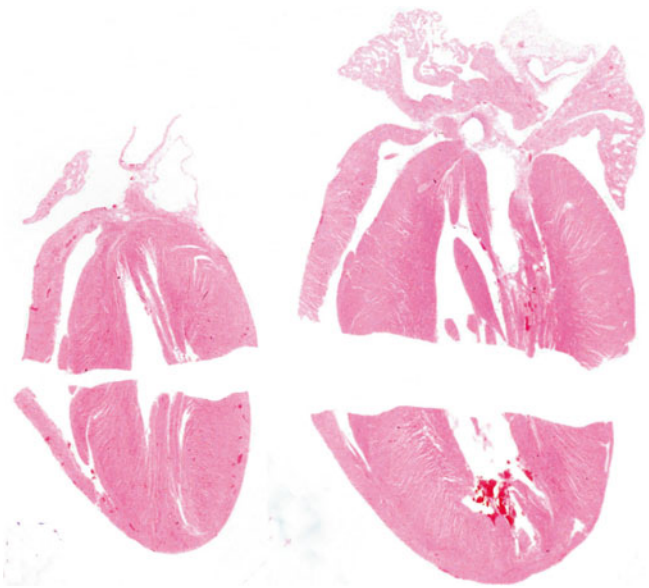

Figure 1-34. Myocardial hypertrophy, left ventricle, on a rat, with no change in histological appearance of individual fibres. H&E.

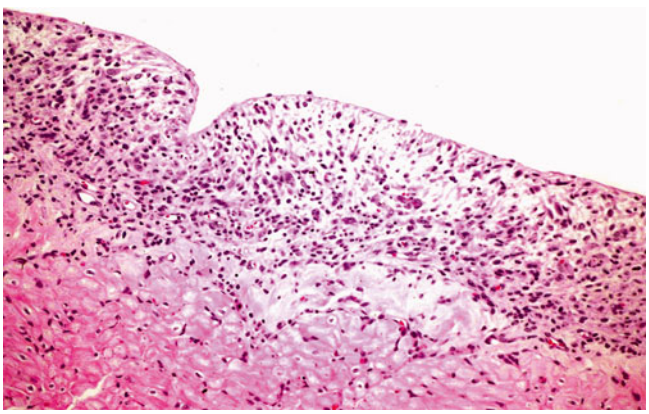

Figure 1-35. Epicarditis, left ventricle, in a dog treated with an immunomodulator. Inflammation and oedema of epicardium are present. H&E.

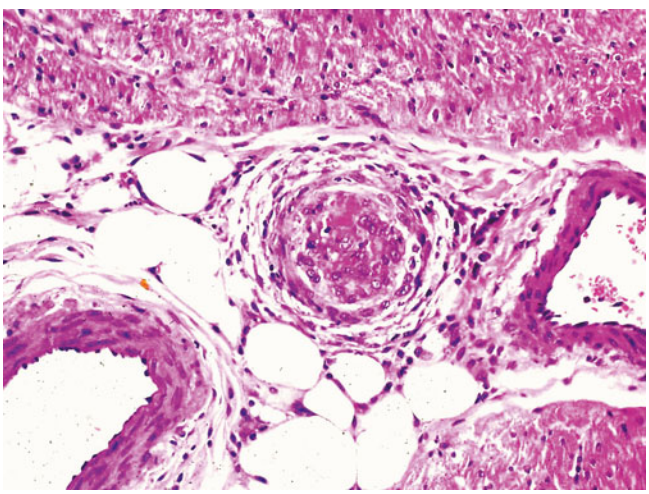

Figure 1-36. Vasculitis, myocardium, of a dog treated with an immunostimulant. Note the intimal proliferation and thrombosis. H&E.

Arteritis and periarteritis of the extramural coronary artery have been recorded in dogs treated with certain immunomodulators. Coronary arterial inflammation was noted in mice treated with an immunomodulator (Fig. 1.40). These lesions in the dog can sometimes be difficult to differentiate from those seen spontaneously in laboratory beagles. Valvular inflammation and stromal proliferation of atrioventricular valves have been noticed in dogs treated with a variety of agents including immunomodulators, biologicals, and certain cardioactive agents (Figs. 1.41 and 1.42) [26–28]. Fat necrosis of epicardial adipose tissue has been seen in dogs treated with novel glucocorticoids (Fig. 1.43) [1]. Atrial thrombosis is sometimes associated with prolonged cases of cardiomyopathy in rodents (Fig. 1.44). Complications in infusion studies can sometimes lead to the development of valvular endocarditis (Fig. 1.45).

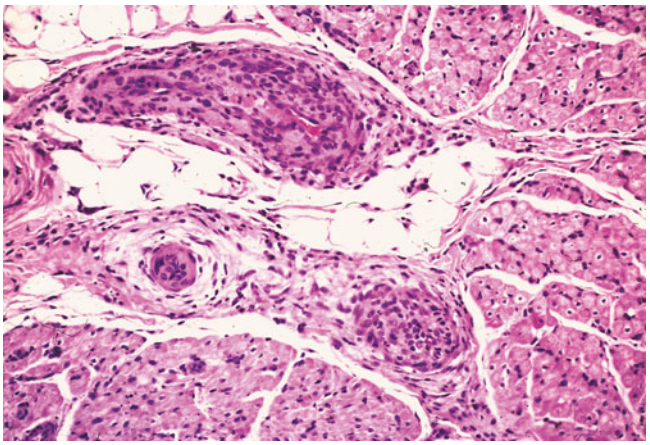

Figure 1-37. Vasculitis and intimal proliferation, coronary artery, in a dog treated with an immunostimulant. Note the luminal occlusion. H&E (With kind permission from Springer Science + Business Media B.V [1]).

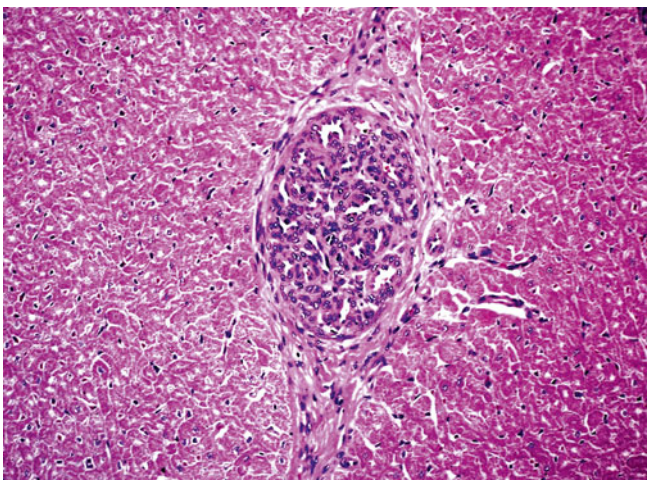

Figure 1-38. Vascular occlusion and recanalisation, myocardial arteries, left ventricle, in a dog treated with an immunostimulant. H&E.

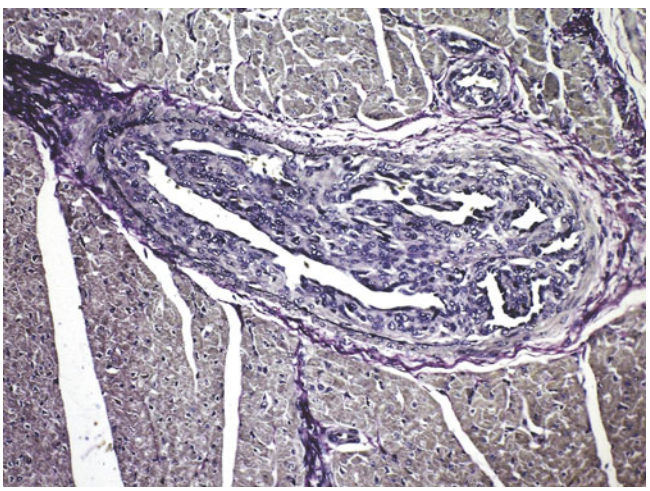

Figure 1-39. Occlusion, myocardial arteries, in a dog treated with an immunostimulant. Note the distinct recanalisation. Elastic van Gieson (With kind permission from Springer Science + Business Media B.V [1]).

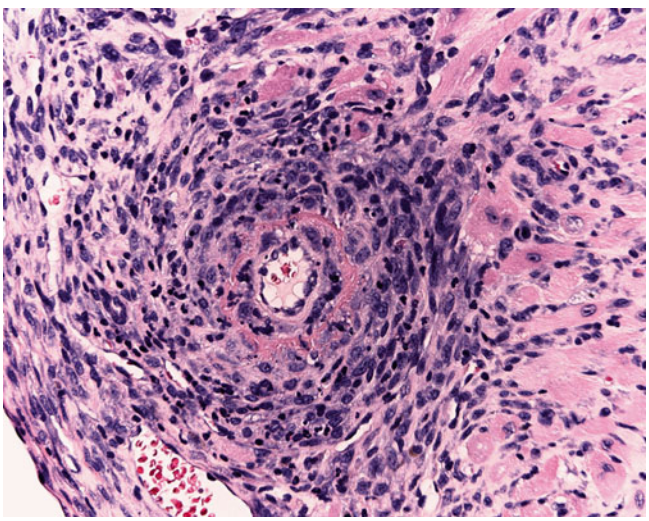

Figure 1-40. Coronary arteritis in a dog treated with an immunomodulator. Note inflammation and necrosis of arterial wall, periarterial inflammation, and fibrosis. H&E.

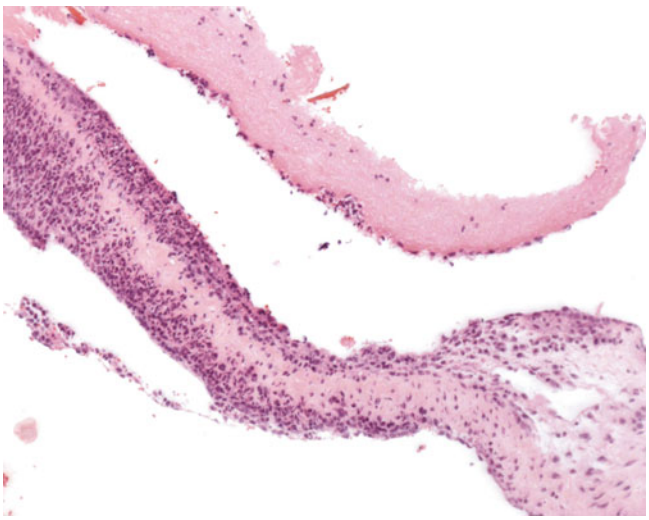

Figure 1-41. Valvular inflammation in a dog treated with an immunomodulator. Note the thickening and inflammatory cell infiltration. H&E.

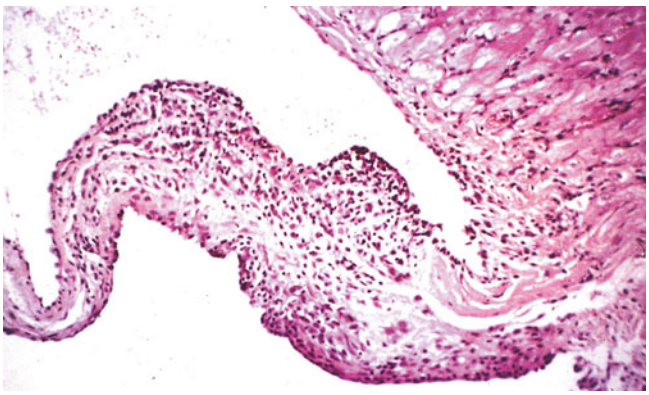

Figure 1-42. Valvular inflammation in a dog treated with an immunomodulator. There is stromal increase and inflammatory cell infiltration causing increased thickness. H&E.

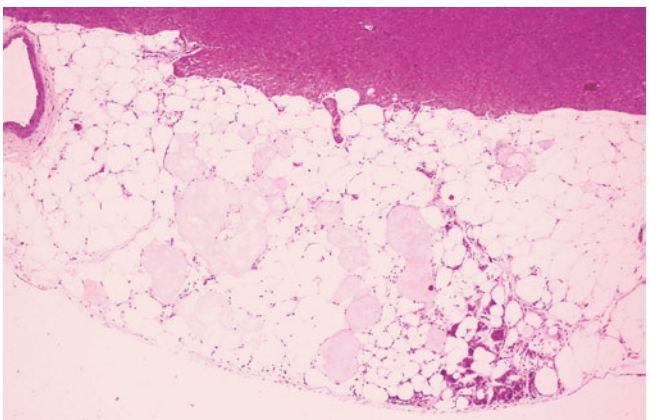

Figure 1-43. Fat necrosis, epicardial fat, in a dog treated with a glucocorticoid agent. H&E (With kind permission from Springer Science + Business Media B.V [1]).

Figure 1-44. Atrial thrombosis in a rat from a chronic toxicity study.

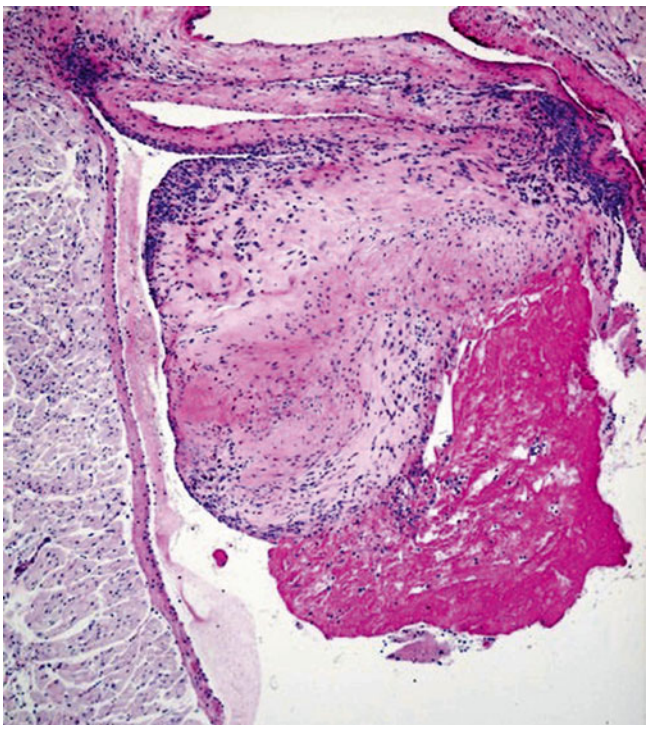

Figure 1-45. Valvular endocarditis, aortic valve, in a dog from an infusion study. The valve is thickened and inflamed and shows thrombosis. H&E.

1.2 Vascular Changes

In addition to the cardiac vessels, peripheral vessels can also become targets in toxicity studies, albeit rarely. Mercury salts induce a vasculopathy in pigs, resulting in degeneration of arteries in meninges, oesophagus, and stomach [29]. The affected arteries show thickening of all layers of the artery, fibrinoid degeneration of the tunica media, and narrowing of the lumen. Monocrotaline, a pyrrolizidine alkaloid, induces occlusive arteritis with thrombosis in the lungs of treated monkeys and rats. Certain immunostimulants have induced necrotising arteritis with extensive inflammation of the periarterial connective tissue in dogs (Fig. 1.46). This type of vasculitis can occur spontaneously in dogs and rodents.

β-Aminopropionitrile causes intramural damage to arteries, with haemorrhage, and can progress to aneurysms in rats [30]. Ergotamine toxicity affects peripheral arteries causing medial degeneration and intimal proliferation. Drug-induced vascular injury (DIVI) in toxicology studies is a frequent problem with several drugs; their mechanisms and extrapolative significance to human safety are poorly understood. Vasodilating antihypertensive agents and PDE inhibitors cause degeneration of the tunica media along with necrosis, inflammation, and haemorrhage, affecting small to medium-sized arteries in experimental animals (Figs. 1.47 and 1.48) [31–36]. The exact location of DIVI is not always predictable, although it frequently affects mesenteric vessels. It is important to note and report the location of affected vessels. Ionotropic vasodilators produce a plexiform vasculopathy in mesenteric vessels (Figs. 1.49 and 1.50) [34]. The affected vessels show intramural vascular channel formation. Thrombosis is often seen with higher incidences in chronic intravenous studies, as a result of direct local effects (Figs. 1.51 and 1.52). Varying degrees of intimal and mural injuries and responses are frequently seen in the vessels of animals used in chronic infusion studies (Fig. 1.53). A novel biotechnological product resulted in adherence of macrophages to the vascular endothelium in the lungs in rats in our laboratories.

Hypervitaminosis D results in widespread and extensive mineralisation of the tunica media of arteries and aorta, sometimes resulting in cartilaginous metaplasia (Fig. 1.54).

Experimental atherosclerosis can be induced in several species. Hyperlipidaemic diets, homocystine, carbon disulphide, and carbon monoxide exposure are known to influence development of atherosclerosis by causing injury to endothelium in experimental animals [1, 37]. Diets rich in cholesterol alone induced atherosclerotic lesions of the coronary arteries, aorta,

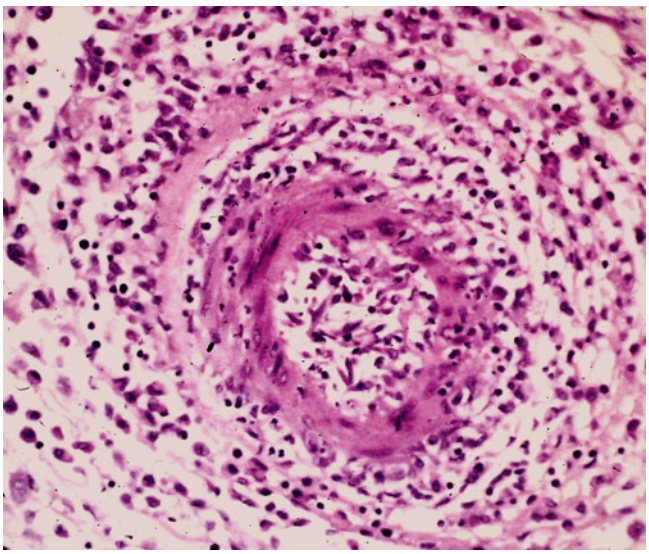

Figure 1-46. Arteritis, coronary artery, in a dog treated with an immunomodulator. Inflammatory cell infiltration of the arterial wall and periarterial connective tissue are noted. H&E.

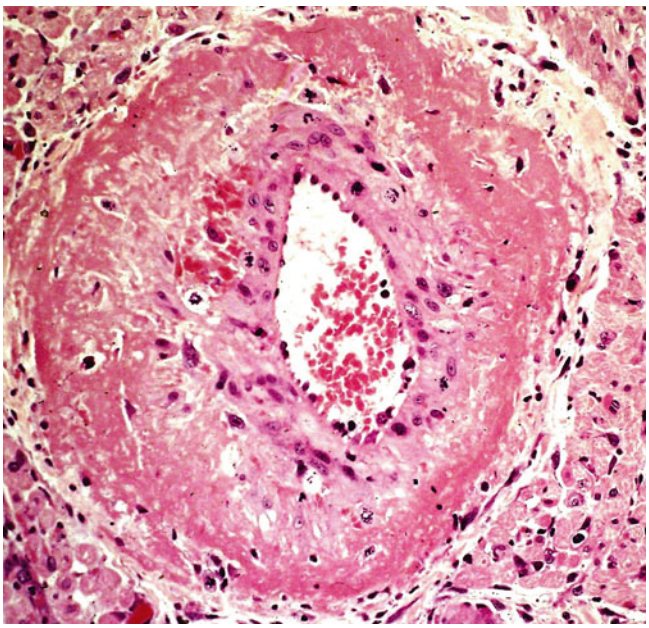

Figure 1-47. Vascular injury, artery, in a dog treated with a phosphodiesterase (PDE) inhibitor. Tunica media reveal necrosis and haemorrhage. H&E.

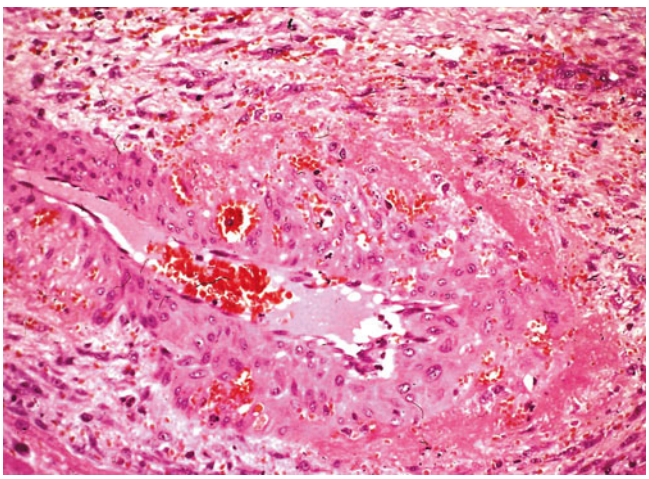

Figure 1-48. Drug-induced vascular injury, artery, in a dog treated with an antihypertensive agent. Arterial wall reveals necrosis, haemorrhage and periarterial inflammation, haemorrhage, and fibroblastic proliferation. H&E.

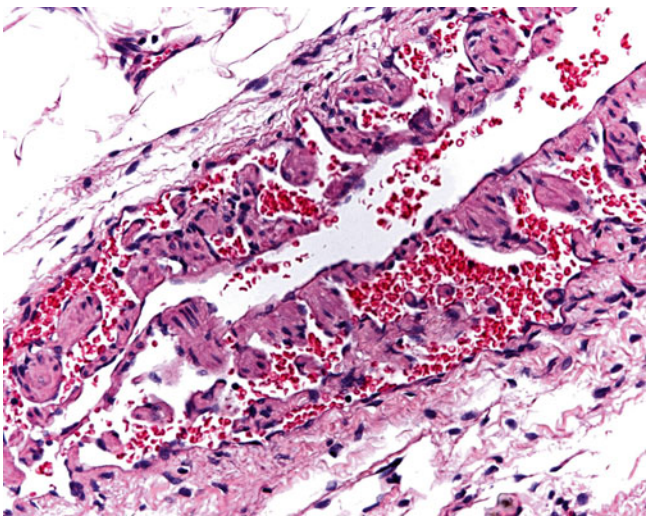

Figure 1-49. Plexiform vasculopathy, mesenteric vessels, in a rat treated with an ionotropic agent. Vessel shows intramural vascular channel formation. H&E.

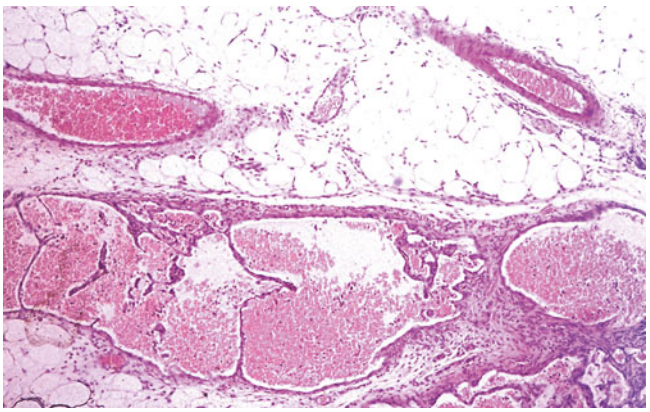

Figure 1-50. Plexiform vasculopathy in a rat. Note the large vascular channels within the mesenteric vessel wall. H&E.

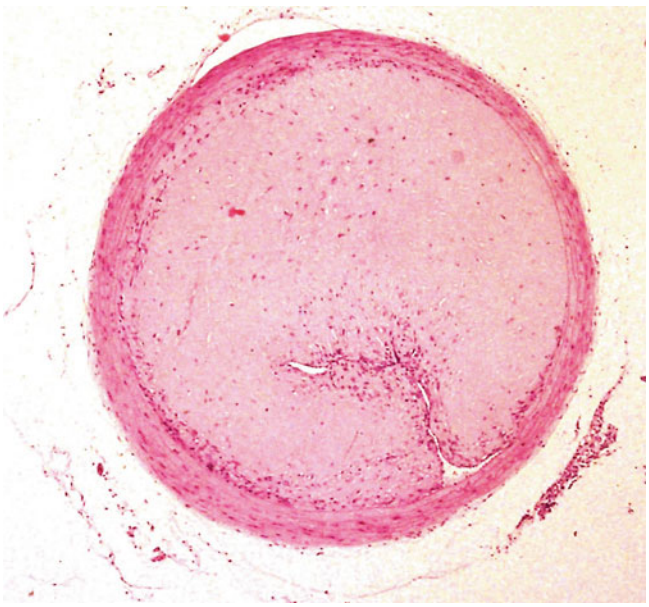

Figure 1-51. Occluding thrombus in a subcutaneous vein at the site of injection. H&E.

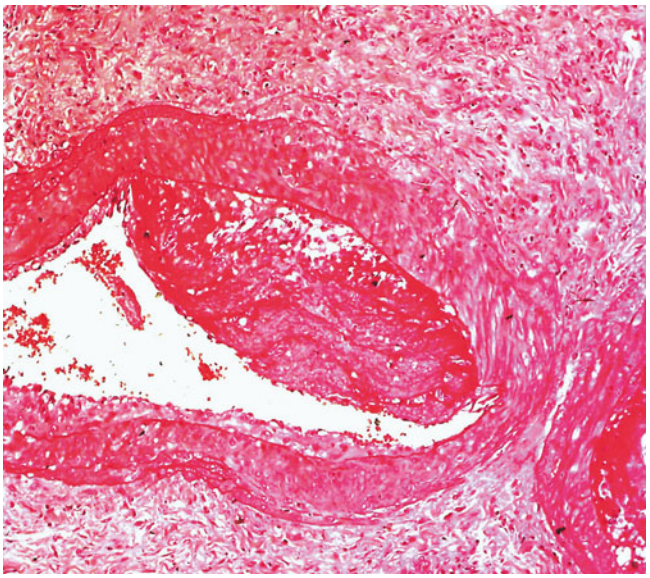

Figure 1-52. Thrombosis at the site of injection in a dog. H&E.

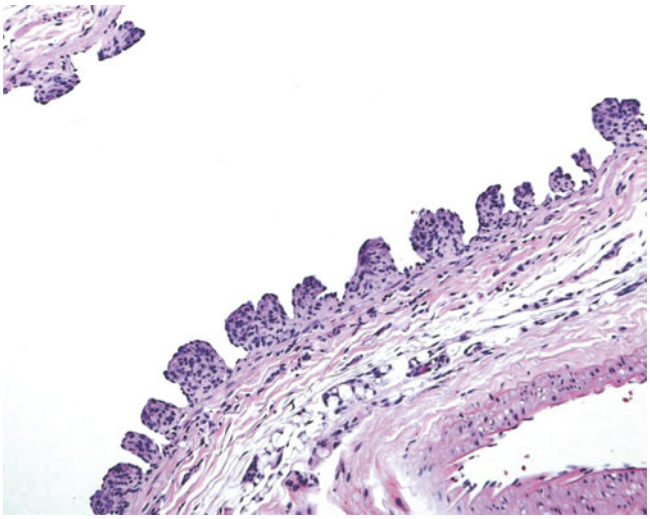

Figure 1-53. Intimal proliferation, multifocal, subcutaneous vessel, in a dog from an infusion study. H&E.

and peripheral vessels in monkeys in our laboratories (Fig. 1.55) [1]. The affected arteries appear thickened, opaque creamy white, and tortuous on the cardiac surface (Fig. 1.56). The affected arteries reveal plaques containing lipoid and mucoid substances along with tissue components such as myofibres, fibroblasts, and macrophages. The plaques are frequently located subendothelially and project into the lumen, causing varying degrees of stenosis (Figs. 1.57 and 1.58). The affected areas show amorphous matrix containing lipid, cholesterol clefts, mucoglycoproteins, calcification, collagen mixed with fibroblasts, smooth muscle cells,

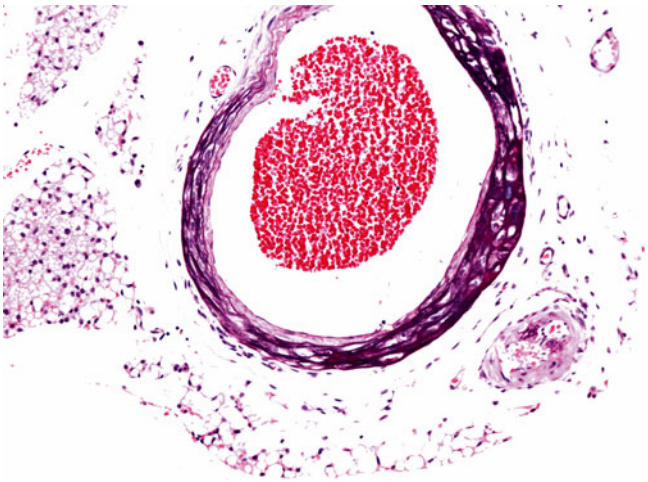

Figure 1-54. Mineralisation and cartilaginous metaplasia, visceral artery, in a rat from a chronic toxicity study with vitamin D analogue. H&E.

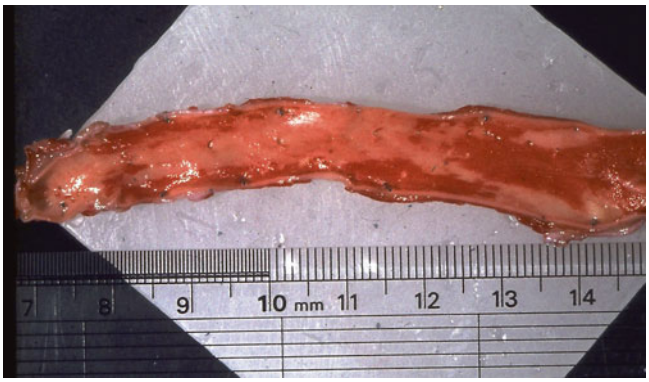

Figure 1-55. Fatty streaks, abdominal aorta, in a monkey. Many raised reddish plaques are seen on the intimal surface. Oil red O (ORO).

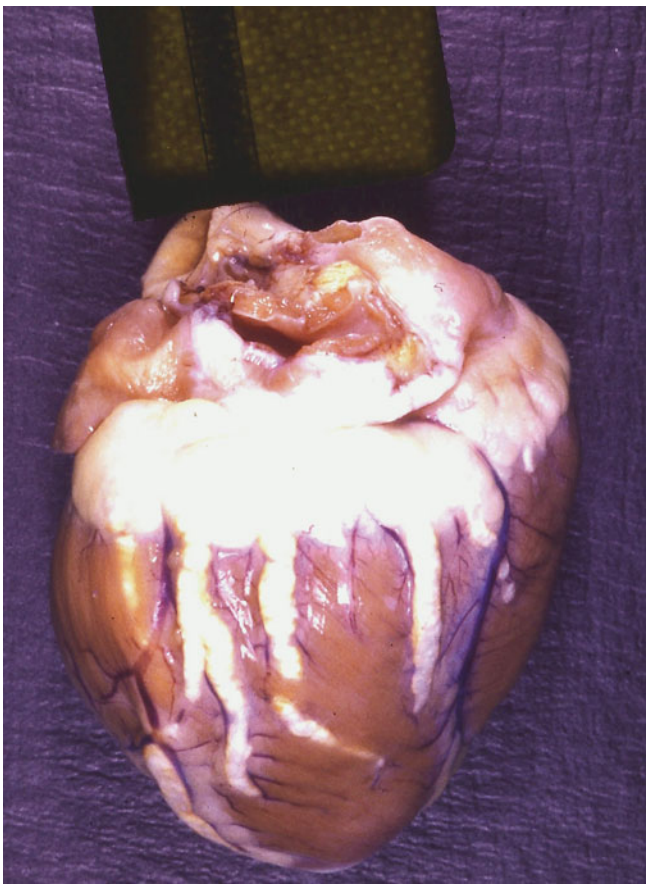

Figure 1-56. Atherosclerosis, coronary arteries, in a monkey. Creamy white coronary arteries appear nodular and thickened.

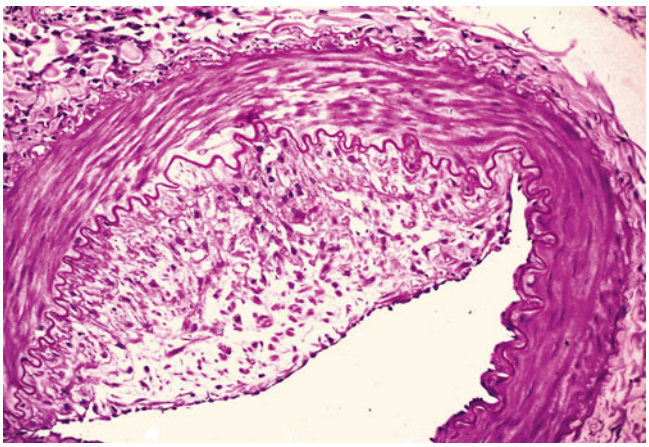

Figure 1-57. Intimal plaque, renal artery, in a monkey. An intimal plaque is present over the internal elastic lamina. H&E (With kind permission from Springer Science + Business Media B.V [1]).

and macrophages. The lesion can extend to involve the tunica media. In extreme cases the lesion can affect all layers. Lymphoid foci were noticed in the tunica adventitia in occasional cases. Ulceration and thrombosis were not recorded in any of the monkeys with atherosclerosis of the coronary arteries.

Vasculitis, mainly affecting medium-sized to small arteries of different organs and tissues, is noted in animals treated with certain PDE-4 inhibitors and other agents (Figs. 1.59 and 1.60). Focal arterial hypertrophy of pulmonary arterioles was seen in rats treated with an industrial chemical (Fig. 1.61).

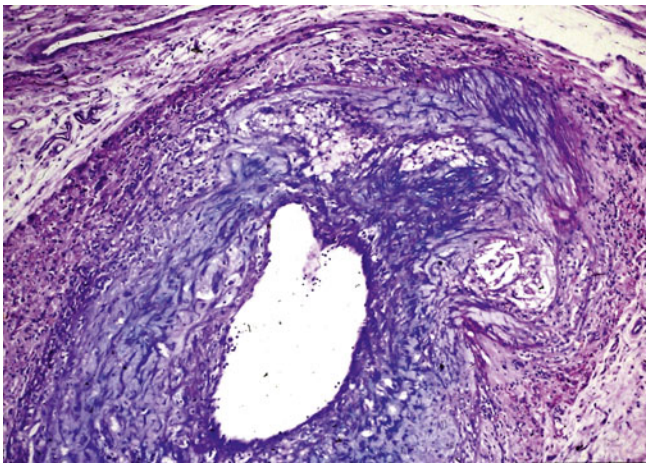

Figure 1-58. Atherosclerotic plaque, coronary artery, in a monkey. Narrowing of the lumen is caused by the plaque with accumulation of mucopolysaccharide in the matrix. Periodic acid–Schiff (PAS)/Alcian blue (With kind permission from Springer Science + Business Media B.V [1]).

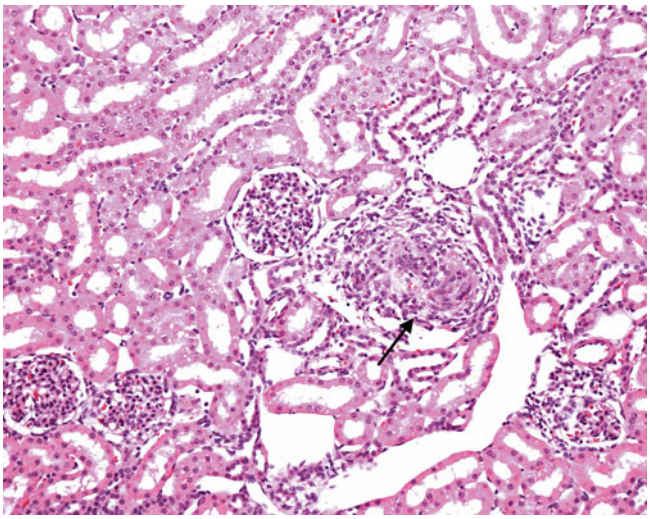

Figure 1-59. Vasculitis, kidney, in a rat treated with a PDE-4 inhibitor shows intramural and perivascular inflammation (*arrow*). H&E.

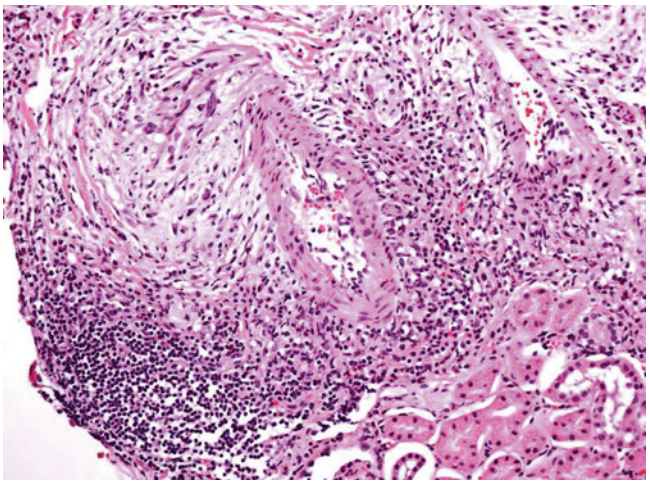

Figure 1-60. Vasculitis in a monkey treated with an immunomodulator. Inflammation of the vessel wall and extensive periarteriolar inflammation and fibroblastic proliferation are seen. H&E.

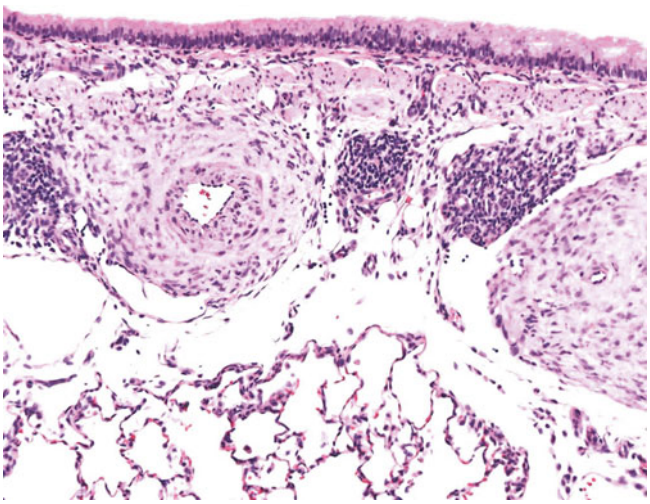

Figure 1-61. Arteriolar hypertrophy, lung, in a rat treated with an industrial chemical. Affected artery shows thickening of the wall and narrowing of the lumen. H&E.

References

1. Gopinath C, Prentice DE, Lewis DJ. The cardiovascular system. In: Atlas of experimental toxicological pathology. Boston: MTP Press Limited; 1987. p. 11–22.
2. Greaves P. Patterns of drug-induced cardiovascular pathology in the beagle dog: relevance for humans. Exp Toxicol Pathol. 1998;50:283–93.
3. Greaves P. Patterns of cardiovascular pathology induced by diverse cardioactive drugs. Toxicol Lett. 2000;112–113: 547–52.
4. Jokinen MP, Lieuallen WG, Boyle MC, Johnson CL, Malarkey DE, Nyska A. Morphologic aspects of rodent cardiotoxicity in a retrospective evaluation of national toxicology program studies. Toxicol Pathol. 2011;39:850–60.
5. Glaister JR. Cardiovascular system. In: Glaister JR, editor. Principles of toxicological pathology. London: Taylor & Francis; 1986. p. 116.
6. Keenan CM, Vidal JD. Standard morphologic evaluation of the heart in the laboratory dog and monkey. Toxicol Pathol. 2006;34:67–74.
7. Herman E, Knapton A, Rosen E, Zhang J, Estis J, Agee SJ, et al. Baseline serum cardiac troponin I concentrations in Sprague–Dawley, spontaneous hypertensive, Wistar, Wistar-Kyoto, and Fisher rats as determined with an ultrasensitive immunoassay 2. Toxicol Pathol. 2011;39:653–63.
8. Walker DB. Serum chemical biomarkers of cardiac injury for nonclinical safety testing. Toxicol Pathol. 2006;34:94–104.
9. Casartelli A, Lanzoni A, Comelli R, Crivellente F, Defazio R, Dorigatti R, et al. A novel and integrated approach for the identification and characterization of drug-induced cardiac toxicity in the dog. Toxicol Pathol. 2011;39:361–71.
10. Balazs T, Earl FL, Bierbower GW, Weinberger MA. The cardiotoxic effects of pressurized aerosol isoproterenol in the dog. Toxicol Appl Pharmacol. 1973;26:407–17.
11. Gopinath C, Thuring J, Zayed I. Isoprenaline-induced myocardial necrosis in dogs. Br J Exp Pathol. 1978;59:148–57.
12. De JS, Verbeeck J, Vinken P, Lammens L, Starckx S, Lachau-Durand S, et al. Hemorrhagic cardiomyopathy in male mice treated with an NNRTI: the role of vitamin K. Toxicol Pathol. 2008;36:321–9.
13. Teske RH, Bishop SP, Righter HF, Detweiler DK. Subacute digoxin toxicosis in the beagle dog. Toxicol Appl Pharmacol. 1976;35:283–301.
14. Gans JH, Korson R, Cater MR, Ackerly CC. Effects of short-term and long-term theobromine administration to male dogs. Toxicol Appl Pharmacol. 1980;53:481–96.
15. Aguirre SA, Heyen JR, Collette III W, Bobrowski W, Blasi ER. Cardiovascular effects in rats following exposure to a receptor tyrosine kinase inhibitor. Toxicol Pathol. 2010;38:416–28.
16. Herman EH, Knapton A, Rosen E, Thompson K, Rosenzweig B, Estis J, et al. A multifaceted evaluation of imatinib-induced cardiotoxicity in the rat. Toxicol Pathol. 2011;39:1091–106.
17. Losco PE, Poulet FM, Kaminska-McNamara GZ, Klein MF. Myocardial and reproductive system toxicity of SCH 351591, a selective phosphodiesterase-4 inhibitor, in CD-1 mice. Toxicol Pathol. 2010;38:568–82.
18. Smith HA. The pathology of gossypol poisoning. Am J Pathol. 1957;33:353–65.
19. Van Vleet JF, Ferrans VJ. Myocardial diseases of animals. Am J Pathol. 1986;124:98–178.
20. Jaenke RS. An anthracycline antibiotic-induced cardiomyopathy in rabbits. Lab Invest. 1974;30:292–304.
21. Billingham ME, Mason JW, Bristow MR, Daniels JR. Anthracycline cardiomyopathy monitored by morphologic changes. Cancer Treat Rep. 1978;62:865–72.
22. Boor PJ, Moslen MT, Reynolds ES. Allylamine cardiotoxicity: I. Sequence of pathologic events. Toxicol Appl Pharmacol. 1979;50:581–92.
23. Greaves P, Martin J, Michel MC, Mompon P. Cardiac hypertrophy in the dog and rat induced by oxfenicine, an agent which modifies muscle metabolism. Arch Toxicol. 1984;7: 488–93.
24. Breider MA, Gough AW, Haskins JR, Sobocinski G, de la Iglesia FA. Troglitazone-induced heart and adipose tissue cell proliferation in mice. Toxicol Pathol. 1999;27:545–52.
25. Sanchez-Soria P, Broka D, Monks SL, Camenisch TD. Chronic low-level arsenite exposure through drinking water increases blood pressure and promotes concentric left ventricular hypertrophy in female mice. Toxicol Pathol. 2012;40:504–12.
26. Donnelly KB. Cardiac valvular pathology: comparative pathology and animal models of acquired cardiac valvular diseases. Toxicol Pathol. 2008;36:204–17.
27. Anderton MJ, Mellor HR, Bell A, Sadler C, Pass M, Powell S, et al. Induction of heart valve lesions by small-molecule ALK5 inhibitors. Toxicol Pathol. 2011;39:916–24.
28. Elangbam CS. Drug-induced valvulopathy: an update. Toxicol Pathol. 2010;38:837–48.
29. Tryphonas L, Nielsen NO. Pathology of chronic alkylmercurial poisoning in swine. Am J Vet Res. 1973;34:379–92.
30. Balazs T, Hanig JP, Herman EH. Toxic responses of the cardiovascular system. In: Klaassen CD, Amdur MO, Doull J, editors. Toxicology. New York: Macmillan; 1986. p. 387.
31. Joseph EC, Rees JA, Dayan AD. Mesenteric arteriopathy in the rat induced by phosphodiesterase III inhibitors: an investigation of morphological, ultrastructural, and hemodynamic changes. Toxicol Pathol. 1996;24:436–50.
32. Joseph EC, Jones HB, Kerns WD. Characterization of coronary arterial lesions in the dog following administration of SK&F 95654, a phosphodiesterase III inhibitor. Toxicol Pathol. 1996;24: 429–35.
33. Joseph EC. Arterial lesions induced by phosphodiesterase III (PDE III) inhibitors and DA(1) agonists. Toxicol Lett. 2000;112–13: 537–46.
34. Westwood FR, Iswaran TJ, Greaves P. Pathologic changes in blood vessels following administration of an inotropic vasodilator (ICI 153,110) to the rat. Fundam Appl Toxicol. 1990;14: 797–809.
35. Weaver JL, Zhang J, Knapton A, Miller T, Espandiari P, Smith R, et al. Early events in vascular injury in the rat induced by the phosphodiesterase IV inhibitor SCH 351591. Toxicol Pathol. 2010;38:738–44.
36. Zhang J, Snyder RD, Herman EH, Knapton A, Honchel R, Miller T, et al. Histopathology of vascular injury in Sprague–Dawley rats treated with phosphodiesterase IV inhibitor SCH 351591 or SCH 534385. Toxicol Pathol. 2008;36:827–39.
37. Wronska-Nofer T, Szendzikowski S, Laurman W. The effect of carbon disulphide and atherogenic diet on the development of atherosclerotic changes in rabbits. Atherosclerosis. 1978; 31:33–9.